Application of RELAP5/Mod3.3 – Fluent coupling codes to CIRCE-HERO

IOP Conf. Series: Journal of Physics: Conf. Series **1224** (2019) 012032 doi:10.1088/1742-6596/1224/1/012032

Application of RELAP5/Mod3.3 – Fluent coupling codes to CIRCE-HERO

N Forgione[1], M Angelucci[1], C Ulissi[1], D Martelli[1], G Barone[1], R Ciolini[1] and M Tarantino[2]

[1] Dipartimento di Ingegneria Civile e Industriale, Università di Pisa, Largo Lucio Lazzarino n. 2, 56122 Pisa, Italy.
[2] ENEA, Cento Ricerche Brasimone, Località Brasimone, 40032 Camugnano (BO), Italy

nicola.forgione@unipi.it

Abstract. This paper presents the work ongoing at the DICI (Dipartimento di Ingegneria Civile e Industriale) of the University of Pisa on the application of coupled methodology between Fluent CFD code and RELAP5/Mod3.3 system code. In particular, this methodology was applied to the LBE-water heat exchanger HERO, with the aim to analyse the performances of this component. The test section object of this study is installed inside the vessel S100 of the CIRCE facility, built at ENEA Brasimone Research Centre.
In the proposed methodology the CFD code is adopted to simulate the LBE side of the HERO heat exchanger, whereas the secondary side (two-phase flow, water-vapour) is simulated by the STH code. In this procedure, the variables exchanged between the boundaries of the two codes are: the bulk temperature and heat transfer coefficient of the ascending water (in two-phase flow) obtained from RELAP5 and transferred to Fluent code; the wall temperature at the water side surface of the pipes is calculated by Fluent and passed to RELAP5 code.
The coupling procedure was verified by comparing the obtained results with the analogous ones achieved with the RELAP5 stand-alone calculation, proving that the developed coupling methodology is reliable. Further, the coupled simulation allows to obtain more accurate information on the LBE side.

1. Introduction

System Thermal-Hydraulic codes (STH) are widely adopted to support the design of components and thermal-hydraulic systems of nuclear power plants (NPP). In particular, these codes are fundamental for nuclear safety analysis as they provide accurate predictions of transients and postulated accidental scenario in NPPs. RELAP5 [1], CATHARE [2], ATHLET [3], TRACE [4], GOTHIC [5], etc. are some of STH codes available to this aim. These codes are also named Best-Estimate (BE) codes because they analyse an accidental scenario as realistically as possible.

STH codes are generally based on one-dimensional form of mass, momentum and energy balance equations, for two-phase flow, solved in Eulerian coordinates, including models based on empirical correlations (e.g. heat transfer, frictional pressure losses, etc.). Currently, their validation has reached a high level of accuracy that allows predicting NPP behaviours within reasonable computational time. However, the STH codes are not suitable to be applied to the study of more complex 3D phenomena

such as, for example, the mixing and thermal stratification phenomena in large pool systems. Indeed, the use of computational fluid dynamics (CFD) has widen its extension in Nuclear Reactor Safety (NRS) field in the last years. These codes reached a satisfactory degree of maturity for single phase flow, particularly in the study of complex 3D phenomena; they combine a refined discretization of the domain with the implementation of models to simulate turbulence, heat transfer, multiphase flows and chemical reactions. However, these advantages involve higher computational efforts compared with those required by the STH codes when applied to an equivalent domain.

In this situation, coupling techniques between STH and CFD codes for thermal-hydraulic analysis purposes appear a good solution to accurately predict the behaviour of NPP components. This methodology allows to obtain different levels of detail in multiscale phenomena. The STH code should be used to simulate system characterized by 1D components (e.g., pipe) and to model multiphase flow, while the CFD code should be used to analyse a smaller part of the domain where 3D effects are significant and/or detailed flow information is demanded.

In this frame, the University of Pisa (UniPi) developed an in-house coupling methodology between the Fluent CFD code and RELAP5/Mod3.3 STH code using a ‘‘non-overlapping scheme”. In particular, the coupling tool was applied to the NACIE experimental loop [6, 7, 8] and the CIRCE experimental pool [8, 9]. These activities were realized in collaboration with ENEA Brasimone RC (Italy), where the facilities have been designed and built.

In the present work, the coupling methodology was applied to the HERO test section, a LBE-water heat exchanger, installed in the CIRCE facility.

2. Coupled codes calculation for thermal-hydraulic analysis of the HERO test section

The ongoing activity is finalized to analyse the heat transfer performance of HERO SGBT (Heavy liquid mEtal – pRessurized water cOoled Steam Generator Bayonet Tube), which is composed by seven double-walls bayonet tubes with a stainless steel powder filling gap. The unit consists of a hexagonal wrap (6795 mm in length) whose inner and outer transversal heights are, respectively, 126 and 132 mm. Six lateral slots are realized in the wrap at the top of the active length (6000 mm) to feed the liquid metal side of the SGBT unit [10].

The performed activity is accomplished using RELAP5 system code coupled with CFD ANSYS Fluent code. In particular, the RELAP5/Mod3.3 is a version modified at the University of Pisa to employ liquid metals, like lead, lead-bismuth and lead-lithium, as working fluids [11]. This coupling approach allows to supply updated and more realistic heat transfer boundary conditions to the CFD model and to obtain more accurate information on heat transfer for this component with a detailed distribution of the LBE temperature inside the hexagonal wrapper.

The adopted methodology for the computational domain is “non-overlapping”. Indeed, the primary side of the heat exchanger and the heat structure are simulated with the CFD code, while the secondary side containing water-vapour two-phase mixture is modelled with the RELAP5 system code.

2.1. CFD preliminary analysis

The CFD preliminary analysis was carried out by ANSYS Fluent solver based on the finite volume method. A 3D model of the LBE side and of the HX solid structures were developed and the mesh was created using the native tool of ANSYS Workbench. Actually, the computational domain is one sixth of the entire geometry in the transversal section, exploiting the symmetry of the section. This simplification reduces the number of elements and as a consequence, the required computational time is decreased. Figure 1(a) shows the overall geometry used in the CFD code calculation, while the details of initial and final regions are displayed respectively Figure 1(b) and Figure 1(c). Figure 2 illustrates the cross section with the description of the different fluid and solid regions reproduced in the model: the LBE part is represented in blue, while the solid structures of AISI-304 steel are depicted in red (the one in contact with LBE side) and green (the one in contact with water side). The AISI-316 powder between the two

steel tubes is coloured in orange. The LBE lateral inlet section is represented in yellow in Figure 1(a) reproducing one of the six entrance slots of the HERO test section.

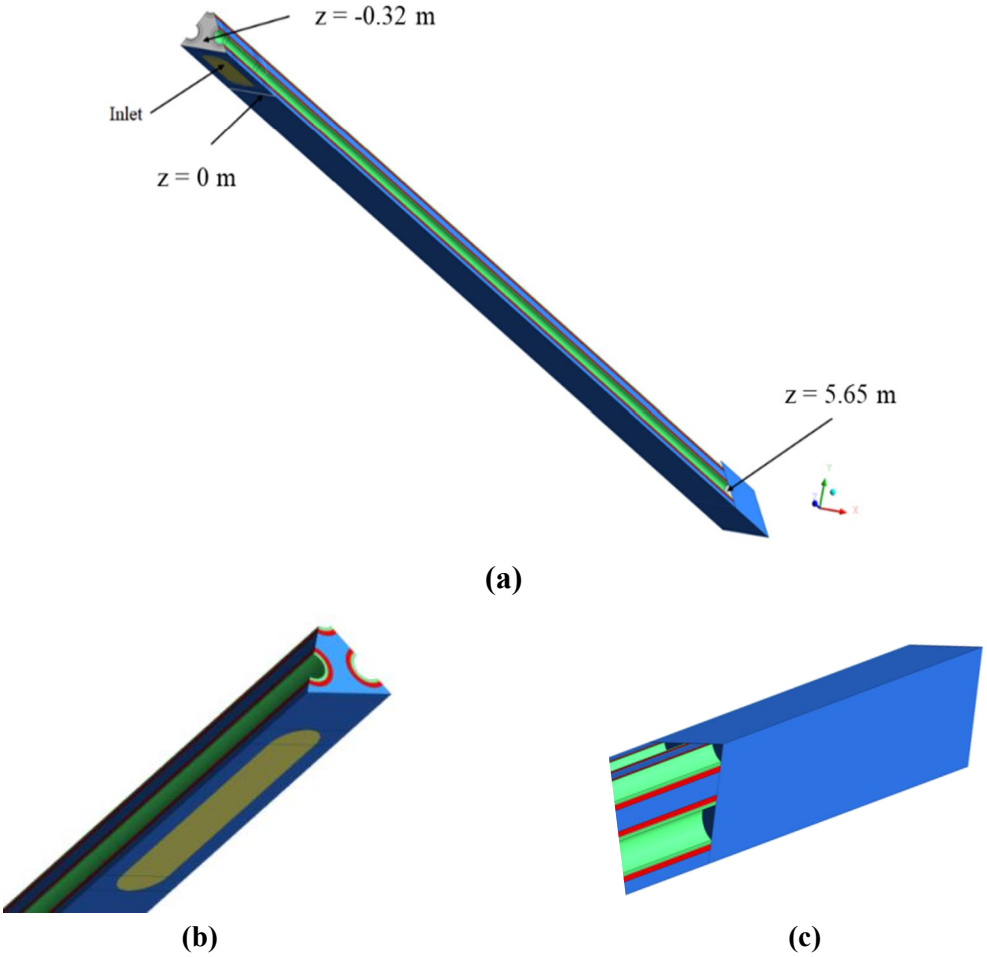

Figure 1. HERO periodic geometrical domain: overall geometry (a), LBE inlet (b) and outlet (c) region.

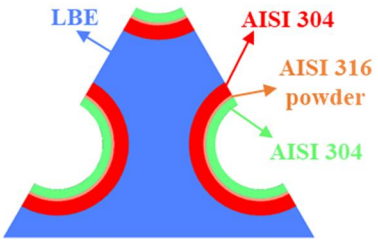

Figure 2. HERO periodic cross section.

The total length was considered including also an LBE zone below the end of the seven water tubes, which was mainly modelled to avoid the "reversed flow" occurrence at the "pressure outlet" boundary condition. This zone is noticeable in the final part of the geometry in Figure 1(c). The spatial discretization, displayed in Figure 3(a) and in Figure 3(b), is characterized by primarily structured hexahedral elements, for a total of 731454 nodes and 688213 elements; additional mesh statistic data are reported in Table 1.

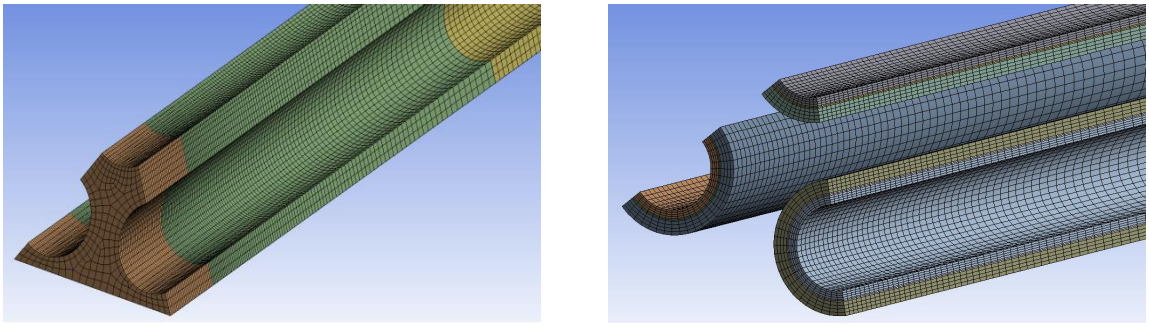

(a) **(b)**

Figure 3. HERO spatial discretization: LBE side (a) and tubes (b).

Table 1. Mesh static data.

Nodes	731454
Elements	688213
Max Aspect Ratio	38.94
Max Skewness	0.79
Min Orthogonal Quality	0.999
Avg Orthogonal Quality	0.983

The LBE properties, such as the density, molecular viscosity, thermal conductivity and specific heat, were taken into account as polynomial functions of the temperature in agreement with OECD/NEA Handbook of 2007 [12]. For AISI-304 steel and AISI-316 powder, the Fluent default values of density and specific heat were adopted, whereas the thermal conductivity of the AISI-304 steel was changed using a polynomial function of the temperature. A constant value of 3.41 W/(m K) was used for the AISI-316 powder, according to Ref. [13]. The thermal properties of solid structures materials are summarized in Table 2 and Table 3.

Table 2. AISI-304 steel thermal properties.

Density, [kg/m^3]	8030
Specific heat, [J/(kg K)]	502.48
Thermal conductivity, [W/(m K)]	9.437+0.0154 T

Table 3. AISI-316 powder thermal properties.

Density, [kg/m^3]	8030
Specific heat, [J/(kg K)]	502.48
Thermal conductivity, [W/(m K)]	3.41

To model heat transfer, the energy equation was activated and the “convection” condition was fixed on the pipe walls. The axial profile of the water side heat transfer coefficient and the two-phase fluid bulk temperature were imposed as thermal wall boundary conditions. The numerical values to apply as

boundary conditions were obtained from a RELAP5 stand-alone simulation. The thermal wall boundary conditions were applied at the inner walls of the ascending water pipes, named Wall 1, Wall 2 and Wall 3, as shown in Figure 4. Different wall boundary conditions between the central pipe (Wall 3) and the lateral pipes (Wall 1 and Wall 2) were adopted, with the aim to obtain more realistic results.

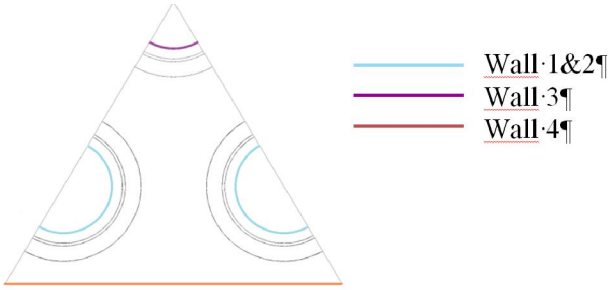

Figure 4. HERO tubes spatial discretization.

In Figure 4, Wall 4 is also shown, which represents the hexagonal wrapper, where no slip and adiabatic conditions were assumed. In addition, the LBE mass flow rate and temperature were imposed at the inlet section, while pressure outlet boundary condition was imposed at the outlet section.

The mesh was developed in agreement with the request of the standard wall function model resulting in $y^+ > 30$ at the wall boundaries. The influence of the adopted turbulence model was also investigated. In particular, three different models were attempted:

- RNG k-ε Model;
- Realizable k-ε Model;
- SST k-ω Model.

The parameters set as boundary conditions at the inlet of the domain summarized in Table 4:

Table 4. Reference boundary conditions.

Inlet LBE mass flow rate, [kg/s]	6.225
Inlet LBE temperature, [°C]	480

The obtained results of LBE temperature, velocity and turbulent kinetic energy (TKE) for the cross section placed at z = 4.1 m are reported in Figure 5, Figure 6 and Figure 7 respectively.

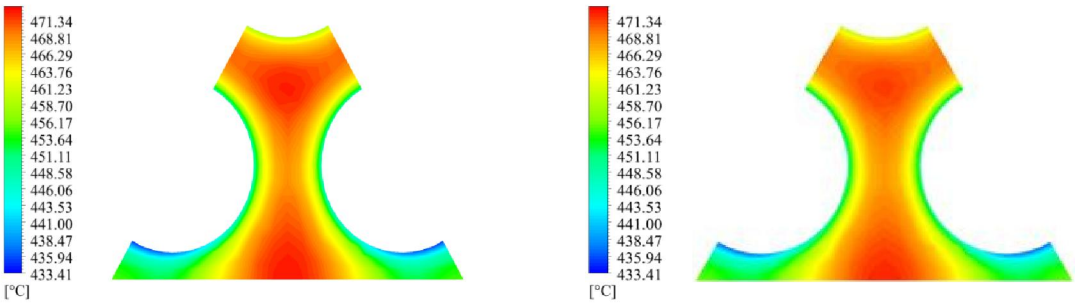

(a) **(b)**

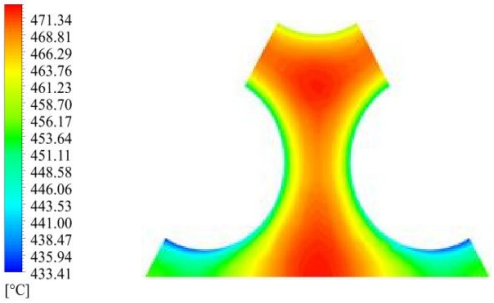

(c)

Figure 5. LBE temperature comparison between the three turbulence models: RNG k-ε Model (a), Realizable k-ε Model (b) and SST k-ω Model (c).

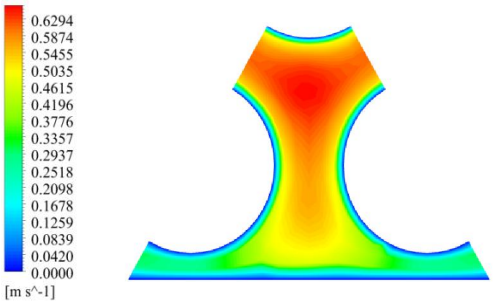

(a)

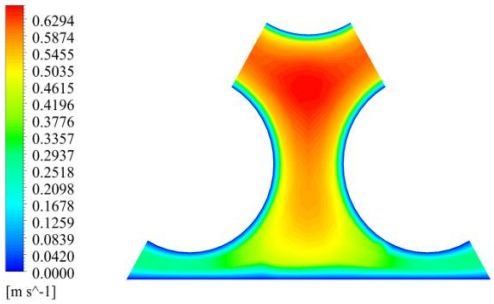

(b)

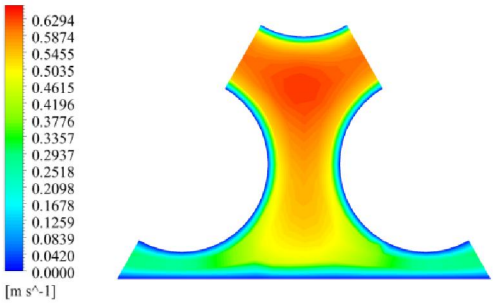

(c)

Figure 6. LBE velocity comparison between the three turbulence models: RNG k-ε Model (a), Realizable k-ε Model (b) and SST k-ω Model (c).

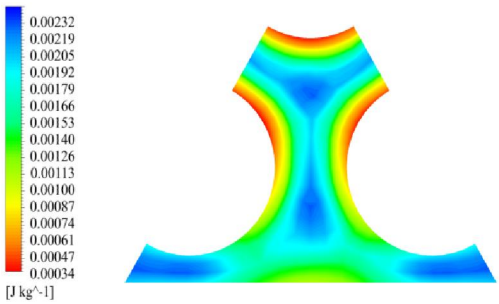

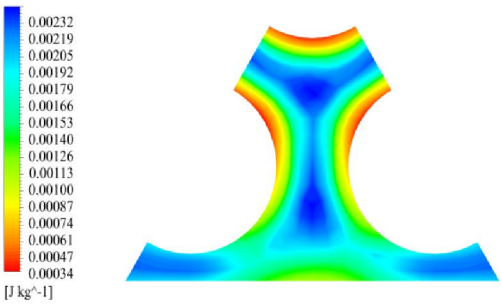

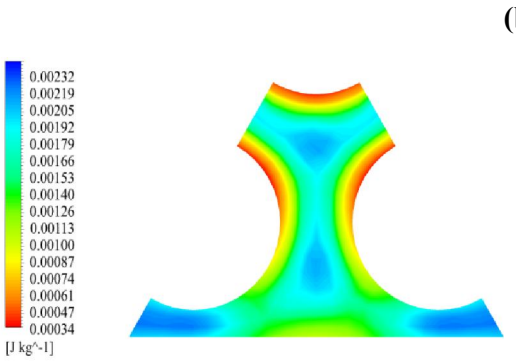

Figure 7 - LBE turbulent kinetic energy comparison between the three turbulence models: RNG k-ε Model (a), Realizable k-ε Model (b) and SST k-ω Model (c).

From Figure 5, Figure 6 and Figure 7, it can be observed that LBE temperature, velocity and turbulent kinetic energy (TKE) distributions are not highly influenced by the adopted turbulence model. In the temperature and velocity profiles, the RNG and Realizable k-ε models show a similar trend while the SST k- ω model results are slightly lower. Instead, the TKE profiles display a more noticeable difference among the models, especially in the SST k-ω model, which generally estimated smaller turbulent parameters. Nevertheless, the choice of the model was based on the comparison of the residual behaviour of the different turbulence models. The model that shows the lowest residuals is the Realizable k-ε model.

Since the turbulent Prandtl number is one of the major parameters affecting sensitively the turbulent heat transfer behaviour in Liquid Metal, additional CFD calculations with Realizable k-ε model were carried out using different turbulent Prandtl number values: 0.85, 1, 1.5 and 2. Changing the turbulent Prandtl number, the LBE temperature profile is slightly different; in particular, higher turbulent Prandtl number gave higher LBE temperature profile over the chosen line.

In absence of experimental data to compare the numerical results and to decide which turbulent Prandtl number is the most appropriate, the choice was based according to the following correlation [14]:

$$Pr_t = \begin{cases} 1.5 & Pe \leq 2000 \\ 2.5 - 0.0005Pe & 2000 \leq Pe \leq 3000 \\ 1.0 & Pe \geq 3000 \end{cases}$$

In the simulated test cases, the Péclet number is generally smaller than 2000, then a Pr_t=1.5 was chosen for the CFD-STH coupled code simulations reported in the next section.

2.2. Adopted coupling procedure

The scheme used for the coupling model is represented in Figure 8, where the thermodynamic variables exchanged at the interfaces between the two domains are highlighted. Basically, the exchange of the variables takes place at the walls of the ascending water pipes along the entire tube length. As already explained, exchanged data are differentiated for the central and the lateral pipes. This differentiation is shown in Figure 8, where the RELAP5 nodalization of the HERO secondary side is reported: the components from 420 to 452 are representative of the central pipe, whereas components from 520 to 552 represent the six lateral tubes. This separation of the central pipe from the lateral ones allows to obtain distinct boundary conditions on the pipes wall from the detailed temperature distribution in the

primary side of the HX (LBE side), calculated by the CFD code. In the RELAP5 model, the water is injected through the time-dependent junction 415 inside the inlet plenum 418 and then redistributes inside the two pipes (420 and 520).

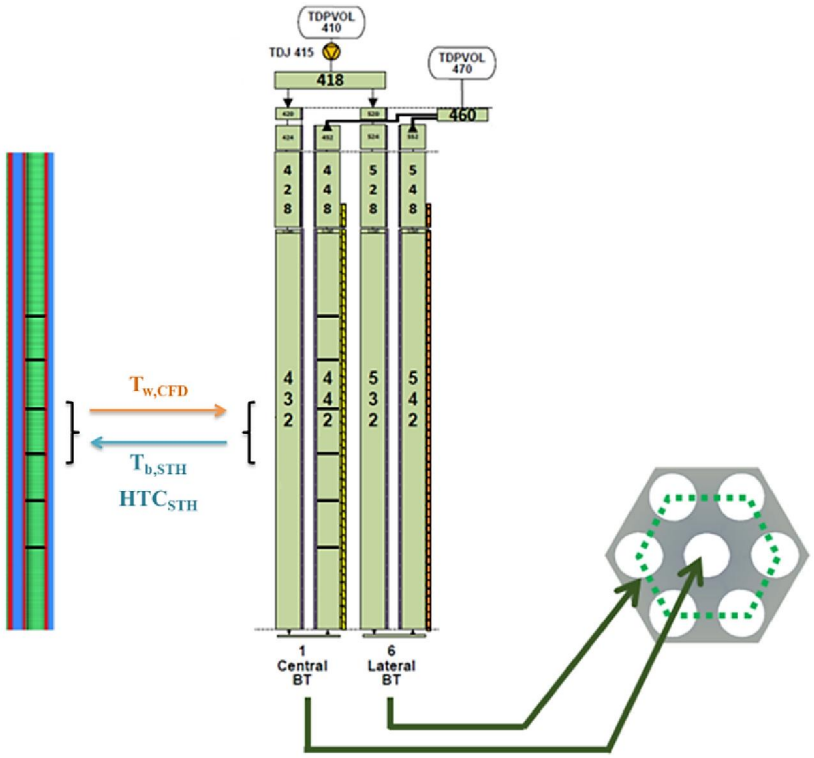

Figure 8. HERO tubes spatial discretization.

60 artificial surfaces have been created on each boundary wall of the CFD domain, in order to exchange data with the system code. The height of these surfaces is equivalent to the respective volume length of pipes 442 (542) and part of pipes 448 (548) of RELAP5. Actually, the divisions are operated on the Wall 2 (the division of Wall 1 is not necessary for symmetry) and Wall 3 because these boundaries are located where the data exchange is carried out between CFD and STH codes. The schematic representation of the artificial subdivision for the data exchange is showed in Figure 8. At each iteration, wall temperature results from Fluent are averaged over the tubes surface (axially and azimuthally) in each of the 60 above-mentioned zones; then these data are transferred to RELAP5. In turn, RELAP5 gives back 60 data points, which are used to build an axial profile (with linear trend between two consecutive points) of both the two-phase water mixture bulk temperature and the Heat Transfer Coefficient (HTC), which are given to Fluent as boundary conditions.

The numerical method adopted for the coupled simulation is the semi-implicit scheme. At each step, for both outer and inner iterations, the variables exchanged between the boundaries of the two codes are:

- the water bulk temperatures;
- the HTC at the pipes wall of the ascending water;
- the wall temperature of the ascending water (in two-phase flow).

The percentage error between the values of each variable at two consecutive iteration is chosen as convergence criteria. More detailed information on the coupling numerical algorithm can be found in Ref. [8].

2.3. Numerical results of HERO coupled calculations

The model for HERO coupled calculations described in section 2.2 was applied to four test cases with the aim to investigate the different performance of the component by changing any of the relevant parameters.

The hydraulic Boundary Conditions (BC) of the HX primary side (LBE) were set in the CFD model and the BCs of the secondary side (water/vapour mixture) were set in the RELAP5 model. The relevant parameters of the four cases are reported in Table 5.

Table 5. Boundary conditions for HERO coupled calculations.

Variable	Case 1	Case 2	Case 3	Case 4
LBE mass flow, [kg/s]	37	9	37	9
LBE inlet temperature, [°C]	480	480	480	480
LBE outlet gauge pressure, [bar]	0	0	0	0
Water mass flow rate, [kg/s]	0.33	0.33	0.08	0.08
Water inlet temperature, [°C]	335	335	335	315
Secondary outlet pressure, [bar]	180	180	180	180

Two different values of the LBE mass flow rate were chosen: the higher one is representative of the normal operating condition of CIRCE, the lower is representative of the natural circulation flow condition typical of CIRCE. Two different levels of water mass flow rate were also investigated, where the higher one is related to the reference design condition.

The characterizing results of the four test cases are summarized in Table 6.

Table 6. Resulting parameters from HERO coupled calculations.

Variable	Case 1	Case 2	Case 3	Case 4
LBE outlet temperature, [°C]	397.8	345.9	455.2	369.9
Water/steam outlet temperature, [°C]	381.3	357.0	478.3	475.0
Outlet static quality, [-]	1	0.38	1	1
Total removed power, [kW]	440	175	132	142

Following the design operating condition, the total power removed by HERO is about 440 kW and this value generally decreased moving from that parameters. Lower LBE outlet temperatures were obtained whenever the LBE mass flow decreased, and almost in all cases the vapour reached superheated conditions.

In the following discussion, Case 1 was chosen for extensive analysis of the results, through the comparison with the analogous RELAP5 standalone calculation. Nevertheless, the RELAP5 standalone model employees a single equivalent water tube to model the 7-tubes of the HERO bundle, which has a total flow area equal to the sum of the individual 7 tube area.

Figure 9 shows the axial trend of temperatures along the HERO test section obtained by the coupling calculation for the central pipe 442 (Figure 9(a)) and lateral pipes 542 (Figure 9(b)). The two images can be compared with Figure 10, which displays the analogous trends obtained with the RELAP5 standalone calculation. The reported profiles depict the trends of LBE temperature, wall temperature on LBE side, the wall temperature on water side and the water temperature both in the descending and ascending tubes.

At first sight, the trends of the temperatures of the central and lateral pipes are similar and there are not evident differences with the RELAP5 stand-alone calculation. Notwithstanding, thanks to the use of coupled calculation it was possible to individuate a slightly different behaviour between the central and the lateral tubes. Indeed, the two-phase flow mixture in the central tube reached the saturated steam condition earlier with respect the lateral tube and the vapour outlet temperature was higher (408.8°C in central pipe versus 378.6°C in lateral pipes). In particular, the CFD portion of the model allows to compute more detailed temperature distribution in the transversal area of the HERO bundle and is able to give to RELAP5 two distinctive boundary conditions respectively to the central and lateral pipes of the bundle.

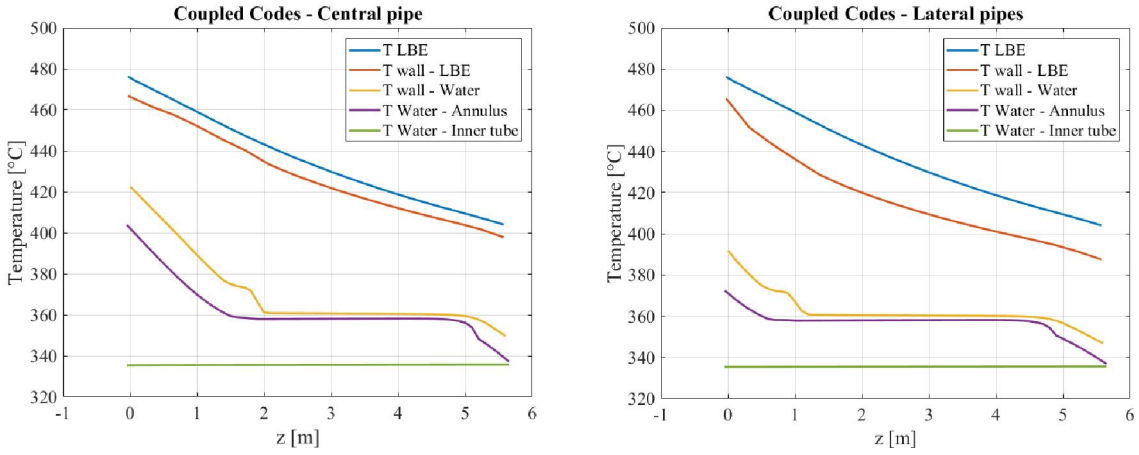

Figure 9. Axial trend of temperatures in the central (a) and lateral (b) pipes from coupled calculation for Case 1.

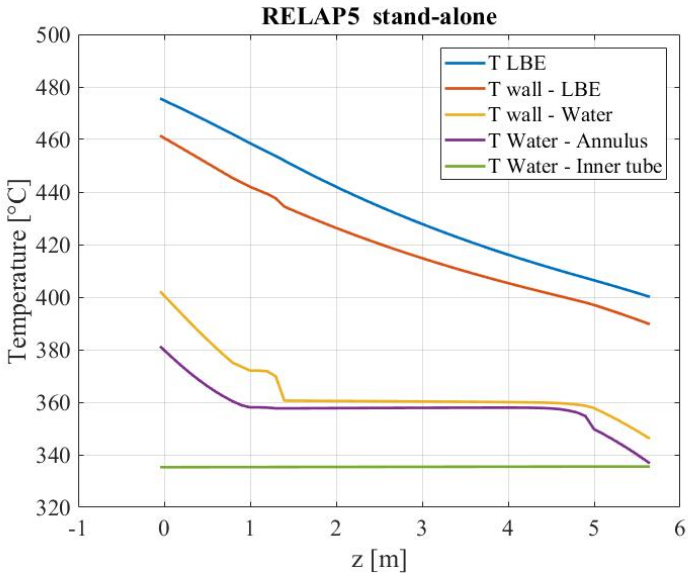

Figure 10. Axial trend of temperatures from RELAP5 standalone calculation for Case 1.

The trends of the HTC of the two-phase flow mixture in the ascending tubes are shown Figure 11, where the results achieved with the coupled calculation (both in central and lateral pipes) are compared

with those obtained from the RELAP5 standalone simulation. The trend of the three curves is very similar; however, the changes in slope occurred in slight different axial positions, according to the temperature trend of the mixture. In particular, it occurs closer to the entrance region in the central pipe than the lateral ones, confirming that the coupled calculation could lead to more accurate information on heat transfer.

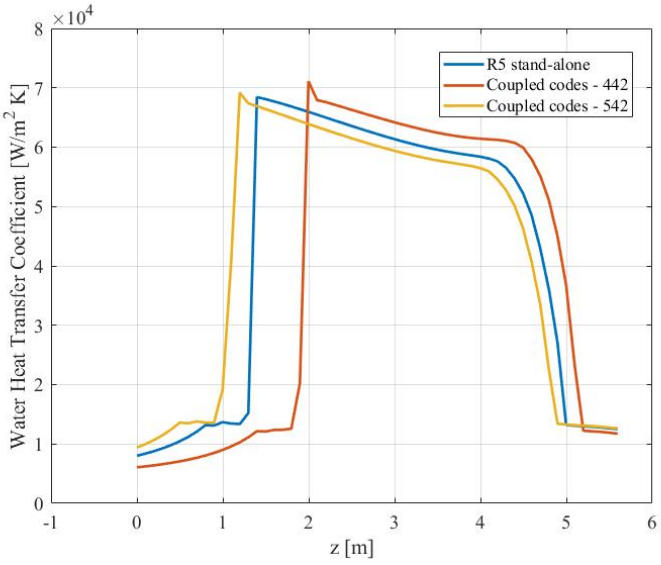

Figure 11. Comparison of the axial trend of HTC – water side for Case 1.

Concerning the value of the HTC in the LBE side, it was possible to obtain the axial trend of HTC directly from the Fluent domain of the coupled model, using the following equation:

$$HTC_{LBE}(z) = \frac{q''_w(z)}{\bar{T}_w(z) - T_b(z)} \quad (1)$$

where q''_w is the wall heat flux, $\bar{T}_w$ is the wall temperature at LBE side and T_b is the LBE bulk temperature. These values were extracted from artificial axial planes specifically created in the CFD domain. In each plane, q''_w and $\bar{T}_w$ were averaged over the total perimeter of both central and lateral walls. In Figure 12, the obtained axial trend is compared with the HTC in the LBE side from the RELAP5 standalone simulation, which was computed using one of the available correlations in the code (Ushakov in this case). The qualitative difference between the two trends is linked to the different way of computing the HTC. In particular, in the CFD calculation it is possible to compute a more detailed variation along the axial coordinate. The initial sharp trend of the curve is related to the entrance region, where the flow and the temperature profile are not developed and the difference between the average wall temperature $\bar{T}_w$ and the bulk temperature T_b is small.

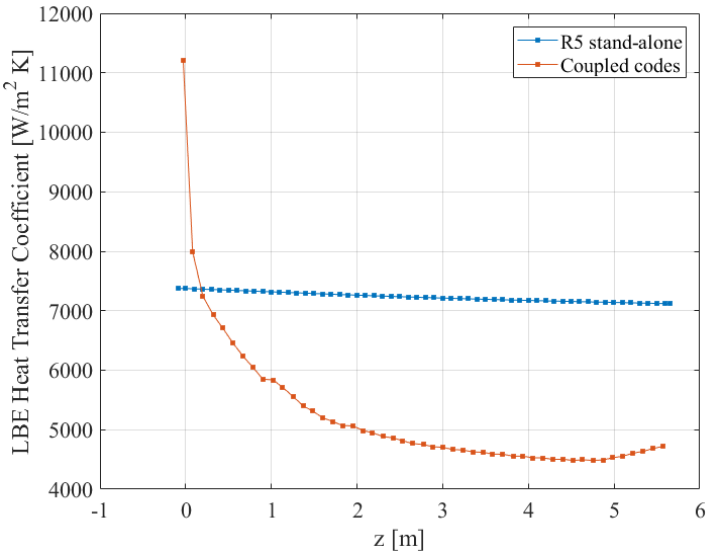

Figure 12. Comparison of the axial trend of HTC – LBE side for Case 1.

As explained in section 2.2, the exchanged heat transfer variables in HERO coupled calculations are the wall temperature (from Fluent to RELAP5) and water/vapour HTC together with the two-phase mixture bulk temperature (from RELAP5 to Fluent). Consequently, the wall heat flux at the boundary walls is computed independently by the two codes. The two heat flux trends, extracted from the Fluent and the RELAP5 domains of the coupled simulation, were compared a posteriori and are illustrated in Figure 13. The two trends are practically coincident over most part of the active length, with exception of few points where the curves have local minimum or maximum. The discrepancy was attributed to limits of the discretization and not to the physical inconsistency. Figure 13(a) and Figure 13(b) show respectively the curves for the central and the lateral tubes, which are put also in comparison with the trend from the RELAP5 standalone calculation.

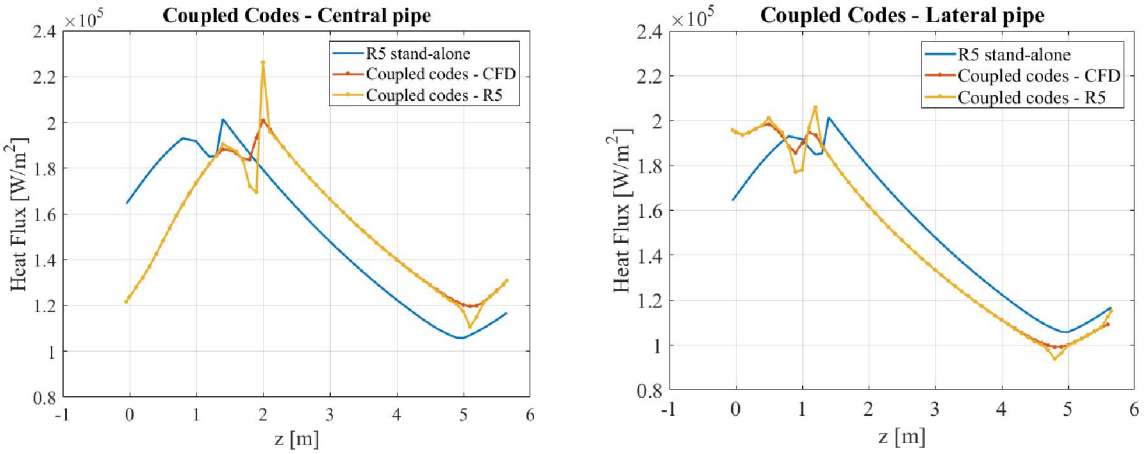

Figure 13. Comparison of the axial trend of the wall heat flux in the central (a) and lateral (b) pipes for Case 1.

The other advantage of using the coupled calculation is the opportunity to analyse more in detail the flow in the portion of the domain modelled by the CFD code. As a showing example, Figure 14 reports

the LBE contour plots for temperature (left) and velocity (right) in three different section, respectively at about z=1.6, 3.6 and 4.1 m. The same scale was used for the three images associated to the same variable. In the contours of temperature, the solid domains (AISI 304 structures and AISI 316 powder) are plotted too. The LBE temperature is colder close to the pipes, where the heat transfer occurs, but also in the outer region between the lateral pipes and the hexagonal wrapper since the LBE velocity is smaller. In the latter region the heat is manly transferred by conduction. Using the same scale range, it is possible to see the different temperature levels during the LBE cooling. The velocity field in the first monitored section (z=1.6 m) appears slightly different with respect to the contour in z=3.6 m and z=5.6 m. Indeed, the first section is still affected by the entrance region and the flow is not completely developed. For the sections z=5.6 m, the flow is finally developed, and the small differences are related to temperature effects.

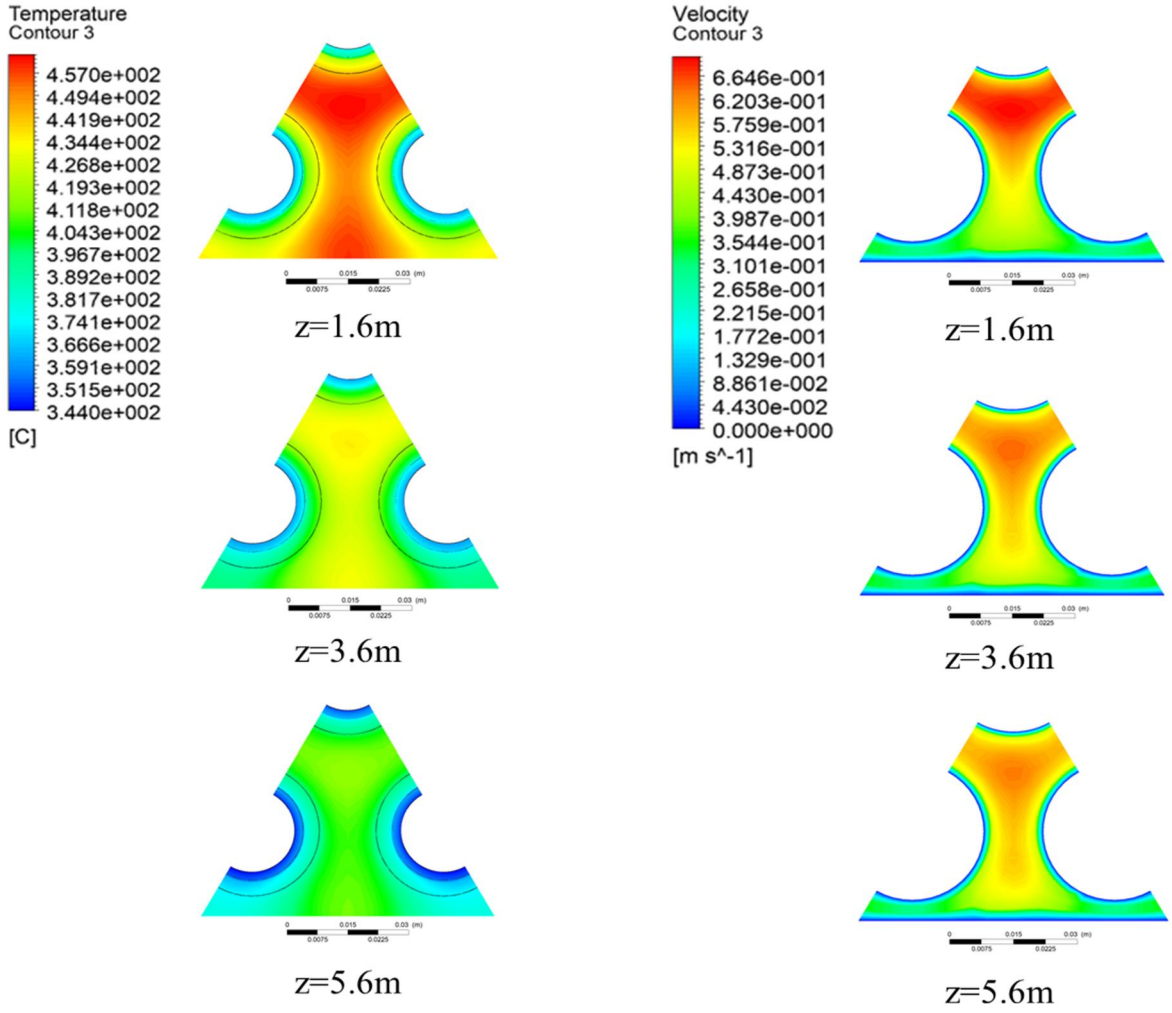

Figure 14. Temperature and velocity magnitude in the LBE side (CFD domain) of HERO at different axial position for Case 1.

3. Conclusions

The present work describes the numerical analysis performed in support of the HERO heat exchanger experimental campaign foreseen at the ENEA Brasimone R.C..

To this end, a coupling methodology between CFD code and system code already developed at the

University of Pisa is improved accounting for its application to thermal boundary conditions.

In the first part of the work, CFD sensitivity analysis were performed in order to select the proper turbulent model and to investigate the effects of the chosen turbulent Prandtl Number. A symmetrical 3D CFD model representative of one sixth of the entire geometry of the LBE side and of the HX solid structures was build.

Boundary conditions, obtained from a previous RELAP5 standalone calculation, were imposed for the CFD standalone calculations (one-way coupling). In particular, the thermal wall boundary conditions were applied at the inner walls of the ascending water.

In the second part of the work, the coupled methodology was applied to the entire HERO section: the primary LBE side and the pipe structures were modelled with the CFD Fluent code whereas the water side was modelled with the STH code RELAP5. The coupling procedure was verified by comparing the obtained results with the analogous ones achieved with the RELAP5 standalone calculation. Similar temperature, heat flux and HTC trends were obtained with the two calculations, proving that the developed coupling methodology is reliable. Further, the coupled simulation allows to obtain more accurate information on the LBE flow and on the heat transfer performance for this component.

As next step, this methodology could be adopted to analyse the performances of the HERO component in several operating conditions (by varying the water side operating pressure, LBE and/or water inlet mass flow rates and temperatures).

At the end of the experimental campaign on the CIRCE-HERO facility, collected detailed experimental data will be use for the verification and preliminary validation of the developed Fluent/RELAP5 coupling mythology in predicting the involved phenomena.

Acknowledgments

This work was performed in the framework of H2020 MYRTE project. This project has received funding from Euratom research and training program 2014-2018, under grant agreement No 662186, and by the Programmatic Agreement (AdP) between the Italian Ministry of the Economic Development (MiSE) and ENEA.

References

[1] Nuclear Safety Analysis Division 2001, RELAP5/Mod3.3 code manual Volume I: Code Structure, System Models, and Solution Methods., vol. 1.
[2] Lavialle G 2006, CATHARE 2 V2.5_1: User's Manual, SSTH/LDAS/EM/2005-035.
[3] ATHLET Mod 3.0 Cycle A. User's Manual, (2012). GRS-P-1/ Vol. 1 Rev. 6 – GRS, Garching bei München, Germany.
[4] TRACE V5. 0, 2007.Theory Manual - Field Equations, Solution Methods, and Physical Models, USNRC, Washington DC.
[5] GOTHIC Thermal Hydraulic Analysis Package User Manual, Version 8.0 (QA), NAI 8907–02, Rev. 20, Numerical Applications Inc., 2012.
[6] Martelli D, Forgione N, Barone G and Di Piazza I 2017, *Coupled simulation of the NACIE facility using RELAP5 and ANSYS FLUENT codes*, Annals of Nuclear Energy 101, 408-418.
[7] Martelli D, Forgione N, Barone G, Del Nevo A, Di Piazza I and Tarantino M, C*oupled simulations of natural and forced circulation tests in NACIE facility using RELAP5 and Ansys Fluent codes*, Proceedings of the 2014 22nd International Conference on Nuclear Engineering ICONE22, July 7-11, 2014, Prague, Czech Republic.
[8] Angelucci M, Martelli D, Barone G, Forgione N and Di Piazza I, *STH-CFD codes coupled calculations applied to HLM loop and pool systems*, Science and Technology of Nuclear Installations, Volume 2017, Article ID 1936894.
[9] Narcisi V, Giannetti F, Tarantino M, Martelli D and Caruso G 2017, *Pool temperature stratification analysis in CIRCE-ICE facility with RELAP5-3D© model and comparison with*

experimental tests, Journal of Physics: Conf. Ser. 923 012006,.
[10] Rozzia D, Del Nevo A and Tarantino M, *HERO-CIRCE Configuration*, Report ENEA CI-I-R-166.
[11] Barone G, Forgione N, Martelli D and Ambrosini W 2013, *System codes and CFD codes applied to loop- and pool-type experimental facilities*, RL 1530/2013, CIRTEN Technical Report, University of Pisa.
[12] OECD/NEA 2007, *Handbook on Lead-bismuth Eutectic Alloy and Lead Properties*, Materials Compatibility, Thermal-hydraulics and Technologies.
[13] ENEA 2016. Private communication.
[14] Cheng X and Tak N I 2006, *CFD analysis of thermal–hydraulic behavior of heavy liquid metals in sub-channels*, Nucl. Eng. Des. 236, pp. 1874-1885.